Postprint, In: Proceedings of the 2010 IEEE/RSJ International Conference on Intelligent Robots and Systems (IROS 2010), pages 3798–3803, Taipei, Taiwan, October 2010

Localization of an Omnidirectional Transport Robot Using IEEE 802.15.4a Ranging and Laser Range Finder

Christof Röhrig, Daniel Heß, Christopher Kirsch, Frank Künemund

Abstract*— Automated Guided Vehicles (AGVs) are used in warehouses, distribution centers and manufacturing plants in order to automate the internal material flow. Usually AGVs are designed to transport large and heavy transport units such as Euro-pallets or mesh pallets. Just-in-time inventory management and lean production requires small transportation units to enable one-piece-flow. Furthermore short production cycles require a flexible material flow which can not be fulfilled by continuous material handling devices like belt or roll conveyors. A solution to meet these demands are small mobile robots for material transport which can replace conventional conveyor systems or large AGVs. The paper presents localization and tracking of an omnidirectional mobile robot equipped with Mecanum wheels, which was designed to transport Euro-bins in a distribution center or warehouse. Localization is realized by sensor fusion of range measurements obtained from an IEEE 802.15.4a network and laser range finders. The IEEE 802.15.4a network is used for communication as well as for global localization. Laser range finders are used to detect landmarks and to provide accurate positioning for docking maneuvers. The range measurements are fused in a Monte Carlo Particle Filter. The paper develops a new motion model for an omnidirectional robot as well as a sensor model for IEEE 802.15.4a range measurements. The experimental results presented in the paper show the effectiveness of the developed models.

I. Introduction

Just-in-time inventory management and short production cycles require flexible material flow as well as usage of small transportation units [1]. These demands can be met by using small Automated Guided Vehicles (AGVs) which act as a swarm of mobile robots. Several companies have introduced small AGVs for logistic applications. Examples are “The Kiva Mobile Fulfillment System (MFS)” [2] and “ADAM™ (Autonomous Delivery and Manipulation)” [3]. Inexpensive localization of small AGVs is an important issue for many logistic applications and object of current research activities. The Kiva MFS uses bar codes on the floor which can be detected with a camera by the AGVs [4]. These bar codes specify the pathways and guarantee accurate localization. Drawbacks of this solution are the risk of polluting the bar codes and the need for predefined pathways which restrict the movements of the AGVs.

Another approach in saving cost for localization is the usage of one technology for more than one function. The paper proposes the usage of an IEEE 802.15.4a Wireless Sensor Network (WSN) for communication as well as for global localization and laser range finders for safety as well as for detecting landmarks and local localization. A WSN consists of spatially distributed autonomous sensor nodes for data acquisition. Besides military applications and monitoring physical or environmental conditions, WSN can also be used for localization. To localize a mobile node, called *tag*, there have to be a couple of nodes with fixed and known positions. These nodes are called *anchors*. WSNs have the advantages that they can be used in a wide field of applications and that they are inexpensive and flexible. An overview of applications for WSNs in logistics is given in [5]. Disadvantage of using a WSN for localizing a mobile robot is the relative low accuracy which is insufficient for docking maneuvers.

Fig. 1. Omnidirectional transport robot

Fig. 1 shows the transport robot which was designed and built in the Intelligent Mobile Systems Lab of the University of Applied Sciences and Arts in Dortmund. It can transport bins with Euro footprint (600x400 mm) in manufacturing plants, distribution centers or warehouses. The robot is equipped with four Mecanum wheels in order to provide omnidirectional motion. This makes the robot applicable in environments with narrow passages and corners. The video attachment of the paper shows the omnidirectional motion capabilities of the robot. The robot is equipped with two laser range finders (Sick S300) which provide operational safety.

This paper extends the work presented in [6] and [7] in several ways. A new motion model for omnidirectional robots is developed and evaluated with experiments using a

The authors are with the University of Applied Sciences and Arts in Dortmund, Intelligent Mobile Systems Lab, Emil-Figge-Str. 42, 44227 Dortmund, Germany. Web: www.imsl.fh-dortmund.de, Email: roehrig@ieee.org

This work was supported in part by the research program of the University of Applied Sciences and Arts in Dortmund (HIFF, Project No. 04 001 79).

mobile robot with Mecanum wheels. A Monte Carlo Particle Filter (MCP) filter is used instead of an Extended Kalman Filter (EKF) in order to deal with non Gaussian motion and sensor models. Furthermore laser range finders are used to detect landmarks and to provide the accuracy which is necessary for docking maneuvers. To localize the mobile robot, the distances and angles to landmarks are fused with the range measurements of the WSN. Both measurements are used by a MCP together with dead reckoning information obtained from wheel encoders.

The paper is organized as follows: Sec. II presents related work. An introduction to sensor fusion using MCP is presented in Sec. III. In Sec. III-A, a motion model for omnidirectional robots is developed. A probabilistic model of measurement errors in ranging obtained from IEEE 802.15.4a is developed in Sec. III-B. Experimental results are presented in Section IV. Finally, the conclusions are given in Section V.

II. Related Work

Up to now, several kinds of localization techniques are developed for the use in wireless networks. A review of existing techniques is given in [8]. These techniques can be classified by the information they use. These informations are: Received Signal Strength (RSS), Angle of Arrival (AoA), Time of Arrival (ToA), Round-trip Time of Flight (RToF) and Time Difference of Arrival (TDoA).

The best accuracy with a relative low effort offer range-based techniques. The range-based methods use distances to known anchors to localize a tag. ToA, RToF and TDoA estimate the range between two nodes by measuring the signal propagation delay. To estimate the position of a mobile device with trilateration, the distances to at least three anchors have to be measured. Ultra Wide Band (UWB) offers a high potential for range measurement using ToA, because the large bandwidth ($> 500\,\text{MHz}$) provides a high ranging accuracy [9]. In [10] UWB range measurements are proposed for tracking a vehicle in a warehouse. IEEE 802.15.4a specifies two optional signaling formats based on UWB and Chirp Spread Spectrum (CSS) with a precision ranging capability. Nanotron Technologies distributes a WSN with ranging capabilities using CSS as signaling format. A modification of RToF utilize the nanoLOC WSN from Nanotron Technologies. The features and modifications of the nanoLOC WSN are described in [11]. For the experiments in this work a nanoLOC network is used.

In order to increase the accuracy of wireless localization techniques, sensor fusion with complementary sensors can be used. In [12] sensor fusion of RSSI obtained from a WSN with computer vision is proposed. Sensor fusion of RSSI obtained from Wireless LAN and laser range finder is proposed in [13]. In that paper the authors propose a hierarchical method which uses the Ekahau location engine for room level localization in the first step and a laser range finder for local localization in the second step.

III. Monte Carlo Particlefilter

Distance measurements obtained from IEEE 802.15.4a are noisy due to None-line-of-sight (NLOS) measurements and multi-path fading. To estimate the pose of a mobile robot accurately by using noisy measurements, methods based on the Bayesian filter are used. The Bayesian filter estimates the pose of a mobile robot by using probability density functions which model the measurement errors. An introduction into the Bayesian filter is given in [14]. One method which is based on the Bayesian filter is the Kalman Filter (KF). The KF has approved itself in mobile robots for position tracking. In [6] the Extended Kalman Filter (EKF) is used to track the position of a forklift truck. The EKF is an extension of the KF for non-linear systems. The EKF from [6] is enhanced in [7] to use distance measurements in NLOS environments. In both papers the distance measurements from a tag to anchors of a nanoLOC WSN are used. The KF and EKF rely on the assumption, that motion and sensor errors are Gaussian and that the estimated position can be modeled by using a Gaussian distribution.

Another method which is based on the Bayesian filter is the Particle Filter (PF). A PF can handle position ambiguities and does not rely on the assumption, that motion and sensor errors are Gaussian. Also PF can cope with multi-modal distributions. In a PF, a set S of N samples is distributed in the environment or at known places. A sample s is defined by Cartesian coordinates and an orientation. A widely used PF for mobile robot localization is the MCP, which is described in [15], [16] and [17]. The estimated pose of a mobile robot and its uncertainty about the correctness is represented by samples. MCP consists of two phases: The *prediction phase* and the *update* phase. In the prediction phase, the motion information $\boldsymbol{u}_k$ is applied on each sample s^i_{k-1} $(1 \leq i \leq N)$. The prediction phase is also called *motion model*. The result of the motion model is a new set of samples $\overline{S}_k$ which represents the positions, where the mobile robot could be after executing the movement $\boldsymbol{u}_k$.

In the update phase, the set of distance measurements D_k is used to assign each sample with an importance factor w. The importance factor complies the probability $p(D_k \mid s^i_k, m)$, i.e. the probability of the distance measurements D_k at a point in the environment defined by sample s^i_k and by using the information from the map m. In m positions of anchors and landmarks are stored. The result of the update phase – also called *measurement update* – is the set of samples $\overline{S}_k$ of the prediction phase with the corresponding set of importance weights $w^{[N]}_k$. Both sets together represent the current position likelihood of the mobile robot. After the update phase, the resampling step follows. Inside the resampling step, samples with a low importance weight are removed and samples with a high importance factor are duplicated. The result of the resampling is the set S_k of N samples which represents the current position of the mobile robot. In the next time step, the set S_k is used as S_{k-1}. There are two options to extract the pose of the mobile robot out of the sample set S_k: The first method is to use the average of all samples and the second method is to use the sample with the highest importance factor. MCPs flow chart is shown in Fig. 2.

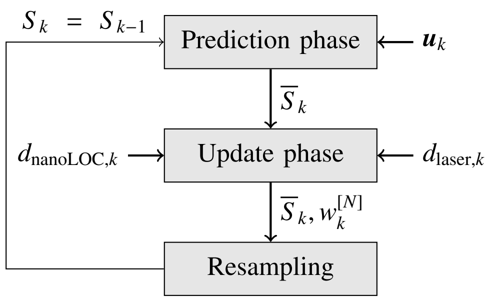

Fig. 2. MCP flow chart.

The MCP has the advantage, that it copes with global localization (no a priori information) and position tracking (given a priori information). Generally the combination of sensor specific advantages and the compensation of sensor specific disadvantages is called sensor fusion. In this paper the MCP fuses distance measurements from nanoLOC WSN and laser range finders.

A. Motion Model for Robots with Mecanum Wheels

A probabilistic motion model is needed in the prediction phase of the MCP. In this section, a new motion model for omnidirectional robots with Mecanum wheels is derived. An omnidirectional robot is able to move in any direction and rotate around its z-axis at the same time. The motion models found in literature are limited to mobile robots with two degrees of freedom. The motion model is based on odometry measurements obtained from wheel encoders. Odometry can be treated as controls, because most robot operating systems control the movements of the robot in a closed position control loop based on odometry. In this case, the command values of the control loop correspond directly to odometry. The movements of the robot are corrupted by disturbances caused by mechanical inaccuracies such as unequal floor contact and slippage. This disturbances will be treated as process noise.

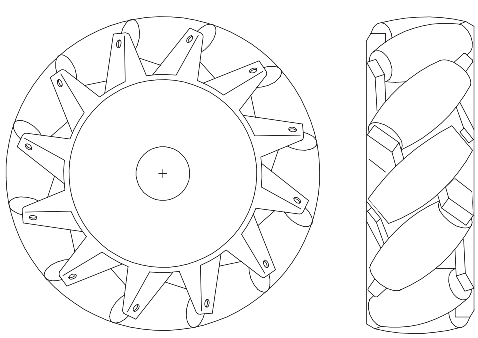

Fig. 3. Mecanum wheel

The mobile robot is equipped with Mecanum wheels and electronic drives, which provide three degrees of freedom. A Mecanum wheel consists of a central hub with free moving rollers, which are mounted at 45° angles around the hubs' periphery (Fig. 3). The outline of the rollers is such that the projection of the wheel appears to be circular. The omnidirectional robot possesses four motor driven Mecanum wheels. The wheel configuration of the mobile system is shown in Fig. 4.

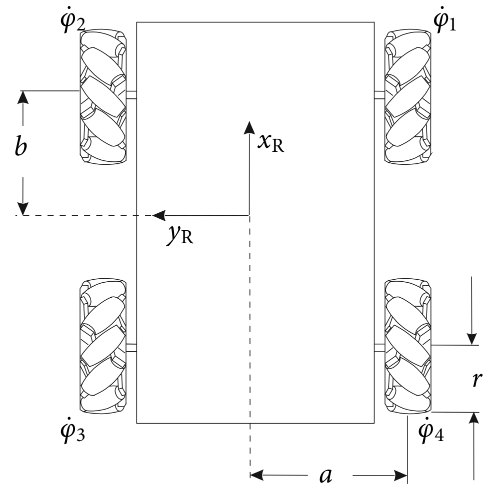

Fig. 4. Omnidirectional robot with Mecanum wheels

The velocities in the robot frame ($\dot{x}_{\mathrm{R}}$, $\dot{y}_{\mathrm{R}}$, $\dot{\theta}$) are a function of the four wheel velocities $\dot{\varphi}_1 \dots \dot{\varphi}_4$:

$$\begin{pmatrix} \dot{x}_{\mathrm{R}} \\ \dot{y}_{\mathrm{R}} \\ \dot{\theta} \end{pmatrix} = \frac{r}{4} \begin{pmatrix} 1 & 1 & 1 & 1 \\ -1 & 1 & -1 & 1 \\ \frac{1}{a+b} & \frac{-1}{a+b} & \frac{-1}{a+b} & \frac{1}{a+b} \end{pmatrix} \begin{pmatrix} \dot{\varphi}_1 \\ \dot{\varphi}_2 \\ \dot{\varphi}_3 \\ \dot{\varphi}_4 \end{pmatrix}, \tag{1}$$

where r is the radius of the wheels, a and b are given by the dimension of the robot (see Fig. 4). Eqn. (1) is used in the operating system of the robot to execute odometry. The inverse equation transforms velocities in the robot frame into the wheel velocities:

$$\begin{pmatrix} \dot{\varphi}_1 \\ \dot{\varphi}_2 \\ \dot{\varphi}_3 \\ \dot{\varphi}_4 \end{pmatrix} = \frac{1}{r} \begin{pmatrix} 1 & -1 & (a+b) \\ 1 & 1 & -(a+b) \\ 1 & -1 & -(a+b) \\ 1 & 1 & (a+b) \end{pmatrix} \begin{pmatrix} \dot{x}_{\mathrm{R}} \\ \dot{y}_{\mathrm{R}} \\ \dot{\theta} \end{pmatrix} \tag{2}$$

Eqn. (2) is used in the operating system of the robot to control the speeds in robot frame. For more details about the kinematics of the mobile robot refer to [18].

Between two time steps of the MCP it is assumed, that the omnidirectional robot moves on a straight line while it rotates from θ_{k-1} to θ_k at the same time (Fig. 5). To simplify calculations, this movement is divided into three independent movements. First a rotation $\Delta\theta/2$, than a translation (Δx, Δy) without rotation and finally again a rotation $\Delta\theta/2$. The movements described in directions of the robot frame can be calculated with (1) as:

$$\begin{pmatrix} \Delta x_{\mathrm{R}} \\ \Delta y_{\mathrm{R}} \\ \Delta\theta \end{pmatrix} = \frac{r}{4} \begin{pmatrix} 1 & 1 & 1 & 1 \\ -1 & 1 & -1 & 1 \\ \frac{1}{a+b} & \frac{-1}{a+b} & \frac{-1}{a+b} & \frac{1}{a+b} \end{pmatrix} \begin{pmatrix} \Delta\varphi_1 \\ \Delta\varphi_2 \\ \Delta\varphi_3 \\ \Delta\varphi_4 \end{pmatrix} \tag{3}$$

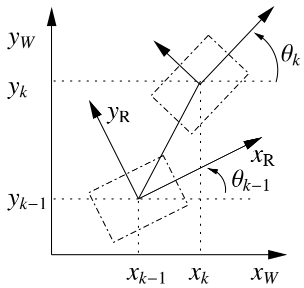

Fig. 5. Movement of an omnidirectional robot

With these movements, the new pose in world frame $\boldsymbol{x}_k = (x_k, y_k, \theta_k)^{\mathrm{T}}$ can be calculated based on the pose before the movement ($\boldsymbol{x}_{k-1}$):

$$\begin{aligned} x_k &= x_{k-1} + \Delta x_{\mathrm{R}} \cos\left(\theta_{k-1} + \tfrac{\Delta\theta}{2}\right) - \Delta y_{\mathrm{R}} \sin\left(\theta_{k-1} + \tfrac{\Delta\theta}{2}\right) \\ y_k &= y_{k-1} + \Delta x_{\mathrm{R}} \sin\left(\theta_{k-1} + \tfrac{\Delta\theta}{2}\right) + \Delta y_{\mathrm{R}} \cos\left(\theta_{k-1} + \tfrac{\Delta\theta}{2}\right) \\ \theta_k &= \theta_{k-1} + \Delta\theta \end{aligned} \tag{4}$$

The movements of the robot are corrupted by noise caused by mechanical inaccuracies. Experiments with the omnidirectional robot show, that the noise is mainly caused by slippage of the Mecanum wheels. Since the slippage of the wheels depends on the rotational speed of the free spinning rollers, the uncertainty depends on the direction of the movement in robot frame. Therefore it is assumed, that the movements of the robot in robot frame are corrupted by independent noise ϵ_i:

$$\Delta\hat{x}_{\mathrm{R}} = \Delta x_{\mathrm{R}} + \epsilon_x \;,\; \Delta\hat{y}_{\mathrm{R}} = \Delta y_{\mathrm{R}} + \epsilon_y \;,\; \Delta\hat{\theta}_{\mathrm{R}} = \Delta\theta_{\mathrm{R}} + \epsilon_\theta \tag{5}$$

Furthermore it is assumed, that the noise ϵ_i is normally distributed with zero mean. The standard deviation σ_i is proportional to the displacement in robot frame:

$$\sigma_x = \alpha_x^x \Delta x_{\mathrm{R}} + \alpha_x^y \Delta y_{\mathrm{R}} + \alpha_x^\theta \Delta\theta_{\mathrm{R}} \tag{6}$$

$$\sigma_y = \alpha_y^x \Delta x_{\mathrm{R}} + \alpha_y^y \Delta y_{\mathrm{R}} + \alpha_y^\theta \Delta\theta_{\mathrm{R}} \tag{7}$$

$$\sigma_\theta = \alpha_\theta^x \Delta x_{\mathrm{R}} + \alpha_\theta^y \Delta y_{\mathrm{R}} + \alpha_\theta^\theta \Delta\theta_{\mathrm{R}} \tag{8}$$

The parameters α_i^j are robot-specific constants.

Usually the operating system of the robot returns odometry values in coordinates of the world frame $\boldsymbol{x}_k^{\mathrm{o}} = (x_k^{\mathrm{o}}, y_k^{\mathrm{o}}, \theta_k^{\mathrm{o}})^{\mathrm{T}}$. In this case, the control value of the sampling algorithm contains odometry values from two time steps $\boldsymbol{u}_k = (\boldsymbol{x}_k^{\mathrm{o}}, \boldsymbol{x}_{k-1}^{\mathrm{o}})^{\mathrm{T}}$, in order to calculate the movement measured by odometry. Algorithm 1 shows the complete sequence of calculations to sample the particles. Lines 2 to 4 calculates the movement in world coordinates, lines 6 and 7 transforms these values in the robot frame. Lines 8 to 10 sample the displacement and 12 to 13 calculate the new pose. The function **sample**(σ) generates normally distributed noise with standard deviation σ.

B. Nanoloc Measurement Model

In the update phase, the measurement model is used to calculate the importance factor w for each sample s. The measurement model is the probability density function $p(d_{\mathrm{nanoLOC},k} \mid s_k^{[i]}, m)$ which characterizes the measurement properties and error. The measurement set $d_{\mathrm{nanoLOC},k}$ contains distance measurements to A anchors. The density function depends on sensors and environment. To estimate the density function for nanoLOC distance measurements, LOS-measurements to four anchors are taken while a mobile robot moves a straight path between them. While the robot moves, the ground truth was estimated by laser measurements to two walls. In Fig. 6, error histograms of measurements to four anchors are shown. The error is the difference between measured distance d_k^a and the Euclidean distance from the robot position to anchor a.

Algorithm 1 Motion sampling algorithm

1: **sample_motion_model($\boldsymbol{u}_k$, $\boldsymbol{x}_{k-1}$)**
2: $\Delta x = x_k^{\mathrm{o}} - x_{k-1}^{\mathrm{o}}$
3: $\Delta y = y_k^{\mathrm{o}} - y_{k-1}^{\mathrm{o}}$
4: $\Delta\theta = \theta_k^{\mathrm{o}} - \theta_{k-1}^{\mathrm{o}}$
5: $\theta' = \theta_{k-1} + \Delta\theta/2$
6: $\Delta x_{\mathrm{R}} = \Delta x \cos\theta' + \Delta y \sin\theta'$
7: $\Delta y_{\mathrm{R}} = \Delta y \cos\theta' - \Delta x \sin\theta'$
8: $\Delta\hat{x}_{\mathrm{R}} = \Delta x_{\mathrm{R}} + \textbf{sample}(\alpha_x^x \Delta x_{\mathrm{R}} + \alpha_x^y \Delta y_{\mathrm{R}} + \alpha_x^\theta \Delta\theta_{\mathrm{R}})$
9: $\Delta\hat{y}_{\mathrm{R}} = \Delta y_{\mathrm{R}} + \textbf{sample}(\alpha_y^x \Delta x_{\mathrm{R}} + \alpha_y^y \Delta y_{\mathrm{R}} + \alpha_y^\theta \Delta\theta_{\mathrm{R}})$
10: $\Delta\hat{\theta} = \Delta\theta + \textbf{sample}(\alpha_\theta^x \Delta x_{\mathrm{R}} + \alpha_\theta^y \Delta y_{\mathrm{R}} + \alpha_\theta^\theta \Delta\theta_{\mathrm{R}})$
11: $\hat{\theta}' = \theta_{k-1} + \Delta\hat{\theta}/2$
12: $x_k = x_{k-1} + \Delta\hat{x}_{\mathrm{R}} \cos\hat{\theta}' - \Delta\hat{y}_{\mathrm{R}} \sin\hat{\theta}'$
13: $y_k = y_{k-1} + \Delta\hat{y}_{\mathrm{R}} \cos\hat{\theta}' + \Delta\hat{x}_{\mathrm{R}} \sin\hat{\theta}'$
14: $\theta_k = \theta_{k-1} + \Delta\hat{\theta}$
15: **return** $\boldsymbol{x}_k = (x_k, y_k, \theta_k)^{\mathrm{T}}$

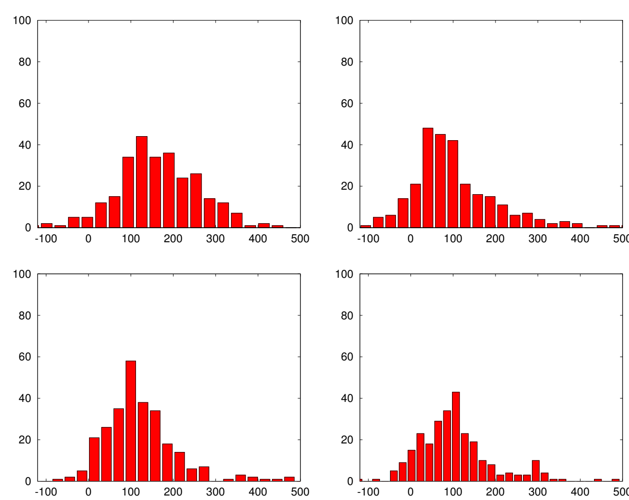

Fig. 6. Error histograms of nanoLOC distance measurements to four anchors. The x-axis is the error in centimeter and the y-axis show their frequency.

The histograms show, that all measured distances are too large, the average error is 107 cm. The error depends on the position of the anchor and on the environment. The median and standard deviation of the error distributions are different but they all have a Gaussian structure. Owing to that fact, it is possible, to use a Gaussian distribution as nanoLOC probability density function:

$$\mathcal{N}\left(x,\mu,\sigma^2\right) = \frac{1}{\sqrt{2\pi\sigma^2}} \exp\left(\frac{-1}{2}\frac{(x-\mu)^2}{\sigma^2}\right) \tag{9}$$

To calculate the importance weight of sample $s_k^{[i]}$, the Euclidean distance $d_k^{a,i*}$ between this sample and the anchor a is calculated as

$$d^{\mathrm{a,i}*} = \sqrt{(x_i - x_a)^2 + (y_i - y_a)^2}, \tag{10}$$

where (x_a, y_a) is the position of Anchor a and (x_i, y_i) are the Cartesian coordinates of sample $s_k^{[i]}$. The Euclidean distance and the measured distance $d_k^{[a]}$ are used with an anchor specific constant d_{const}^a in a fixed Gaussian distribution:

$$p\left(d_{\mathrm{nanoLOC},k} \mid s_k^{[i]}, m\right) = c_1 \mathcal{N}\left(d^{a,i*} - (d_k^{[a]} - d_{\mathrm{const}}^{[a]}), 0, \ \sigma^2\right) \tag{11}$$

where d_{const}^a is the median of the distance errors shown in the histograms. The advantages of this fixed Gaussian distribution are, that a normalization during the localization, to guarantee $\sum p = 1$, is not needed and that the domain can be restricted. This last advantage can be used to detect estimation failure. If a lot of samples are out of range, new samples can be drawn in the environment. This fact enables the MCP to re-localize the mobile robot.

The importance factor of a sample is calculated with:

$$w_k^{[i]} = \prod_{a=1}^{A} p\left(d_{\mathrm{nanoLOC},k}^{[a]} \mid s_k^{[i]}\right) \cdot \prod_{l=1}^{2} p\left(d_{\mathrm{laser},k}^{[l]} \mid s_k^{[i]}\right) \tag{12}$$

The importance factor w is the product of the probability of measurements to A anchors and to two landmarks. The probability $p(d_{\mathrm{laser},k}^l | s_k^{[i]}, m)$ is a fixed Gaussian with $\sigma = 100\,\mathrm{mm}$. The landmarks are equipped with reflectors, in order to allow easy detection by the laser range finders. If no landmarks are detected, the importance factor is equal the probability of the distance measurements to A anchors.

IV. Experimental Results

To evaluate the proposed MCP localization, some experiments are conducted at the University of Applied Sciences and Arts in Dortmund. The mobile robot is equipped with two Sick 300 laser range finders with a scanning angle of 270°. With both laser range finders, the robot gets a full 360° scan of the environment. The laser range finders provide a resolution $\Delta\alpha$ of 0.5°. A docking station for hand over of bins serves as landmark. Two pillars of the docking station are equipped with reflectors, in order to allow easy detection by the laser range finders. The mobile robot is equipped with a nanoLOC tag for ranging and communication purposes. At the margins of the environments six nanoLOC anchors are placed.

The robot is moved in manual mode from a starting point into the docking station. Fig. 7 shows the trajectory along with the results from MCP. The movements starts at the position in the lower left corner. The robot is moved forward first, then sidewards and finally forwards into the docking station in the upper right corner of Fig. 7. During

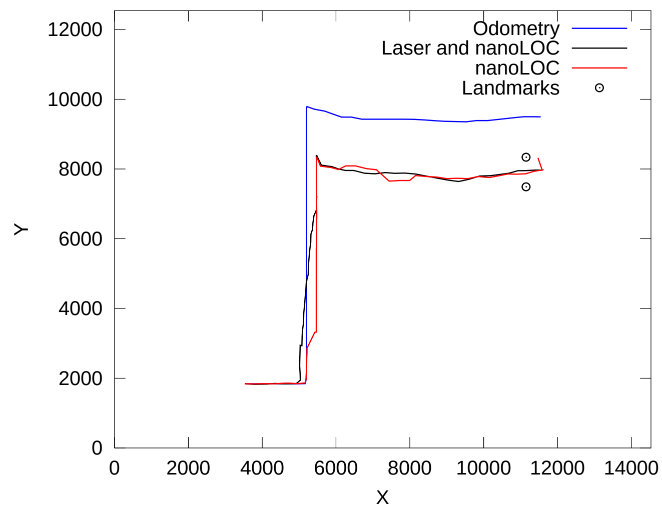

Fig. 7. Position estimation using different sensors.The x- and y-axis of the environment is scaled in mm.

the movement of the robot, all necessary sensor date for MCP are stored. These values are the odometry data, distance measurements to six nanoLOC anchors and the laser range data. The main localization task for mobile robots is position tracking. To perform this task, the MCP starts with 1000 samples at a known position with correct orientation. Owing to an unequal floor contact, the robot has a large slippage, when it moves sideways. Fig. 7 shows odometry in blue, MCP estimation using nanoLOC only in red and MCP using all sensor data in black.

The sample clouds of position tracking are shown in Fig. 8. In part a) the MCP uses only range data obtained from IEEE 802.15.4a network. Part b) shows tracking and sample clouds when using IEEE 802.15.4a as well as both laser range finders. In part a) the particle clouds have a larger vertical extent than in part b) where laser range finders are used. In both parts, the vertical extent of the sample clouds is very large, when the robot moves sideways. This uncertainty is mainly caused by the high slippage in the y_{R}-direction of the robot and y-direction of the world frame in Fig. 8. This uncertainty is modeled by process noise and parameter α_y^y, which has a significantly higher value than α_x^x. The extent of the sample clouds is smaller, if laser range finders are used. This fact is caused by lower standard deviation of the laser range finders sensor model. At the end of the movement in part a) of Fig. 8, the position estimate steps in y-direction of the world frame. This step is caused by NLOS measurements in the docking station, because the direct line of sight from tag to anchors is blocked in the station.

Experimental results show, that the MCP is able to track the robot's position properly, even if it uses only nanoLOC ranging. Using also laser range data improves the position accuracy and allows docking maneuvers.

V. Conclusions

In this paper, localization and tracking of an omnidirectional mobile robot which was designed to transport Euro-

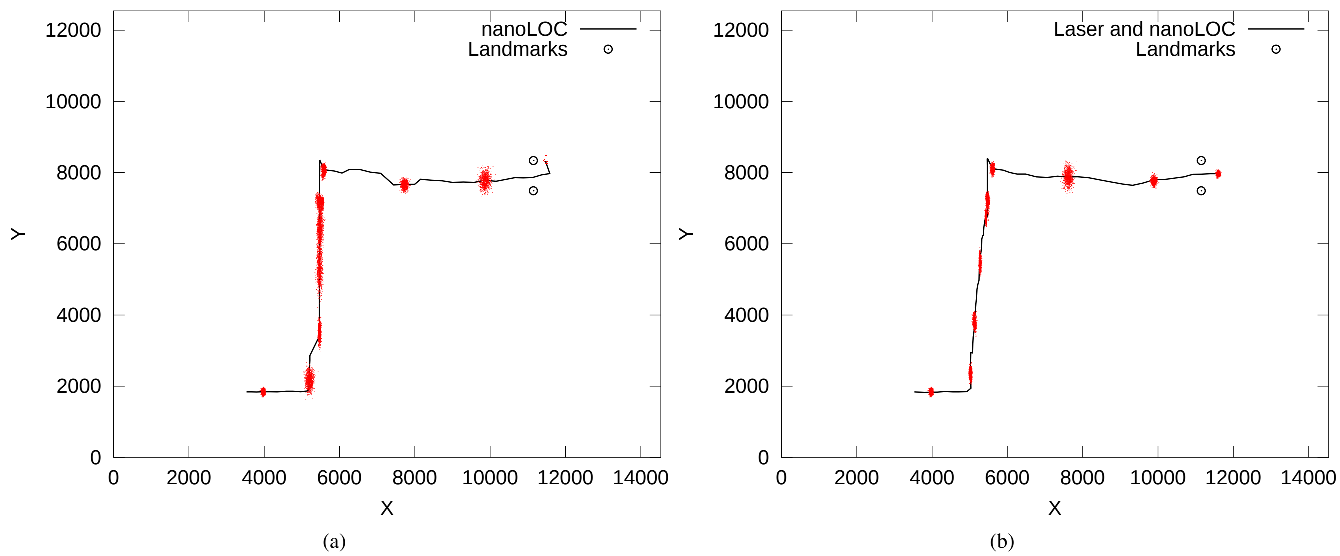

Fig. 8. Tracking of an omnidirectional mobile robot using MCP sensor fusion. a) MCP localization using IEEE 802.15.4a ranging only. b) MCP localization using IEEE 802.15.4a ranging as well as laser range finder. In both pictures, the black line represents the estimated path, the red clouds represent the particles. The x- and y-axis of the environment is scaled in mm.

bins in a distribution center or warehouse is presented. Localization is realized by sensor fusion of range measurements obtained from an IEEE 802.15.4a network and two laser range finders. The range measurements are fused in a MCP. The IEEE 802.15.4a network is used for communication as well as for global localization and two laser range finders are used for safety as well as for landmark detection and local localization. The paper has developed a new motion model for an omnidirectional robot as well as a sensor model for IEEE 802.15.4a range measurements. The structure of the measurement model and the landmark detection process was described.

Experimental results show, that the MCP is able to track the robot's position properly, even if it uses only nanoLOC ranging. Using also laser range data improves the position accuracy and allows docking maneuvers.

References

[1] K. Furmans, M. Schleyer, and F. Schönung, "A Case for Material Handling Systems, Specialized on Handling Small Quantities," in *Proceedings of the 10. International Material Handling Research Colloquium (IMHRC 2008)*, Dortmund, Germany, May 2008.

[2] Kiva Systems, "The Kiva Mobile Fulfillment System (MFS)," http://www.kivasystems.com.

[3] RMT Robotics Ltd., "ADAM (Autonomous Delivery and Manipulation)," http://www.adam-i-agv.com.

[4] E. Guizzo, "Three Engineers, Hundreds of Robots, one Warehouse," *IEEE Spectrum*, vol. 7, pp. 27–34, 2008.

[5] L. Evers, M. J. J. Bijl, M. Marin-Perianu, R. S. Marin-Perianu, and P. J. M. Havinga, "Wireless Sensor Networks and Beyond: A Case Study on Transport and Logistics," Centre for Telematics and Information Technology, University of Twente, Enschede, Netherlands, Technical Report TR-CTIT-05-26, 2005.

[6] C. Röhrig and S. Spieker, "Tracking of Transport Vehicles for Warehouse Management using a Wireless Sensor Network," in *Proceedings of the 2008 IEEE/RSJ International Conference on Intelligent Robots and Systems (IROS 2008)*, Nice, France, Sep. 2008, pp. 3260–3265.

[7] C. Röhrig and M. Müller, "Indoor Location Tracking in Non-line-of-Sight Environments Using a IEEE 802.15.4a Wireless Network," in *Proceedings of the 2009 IEEE/RSJ International Conference on Intelligent Robots and Systems (IROS 2009)*, St. Lous, USA, Oct. 2009, pp. 552–557.

[8] M. Vossiek, L. Wiebking, P. Gulden, J. Wieghardt, C. Hoffmann, and P. Heide, "Wireless Local Positioning," *Microwave Magazine*, vol. 4, no. 4, pp. 77– 86, Dec. 2003.

[9] S. Gezici, Zhi Tian, G. Giannakis, H. Kobayashi, A. Molisch, H. Poor, and Z. Sahinoglu, "Localization via Ultra-wideband Radios: A Look at Positioning Aspects for Future Sensor Networks," *Signal Processing Magazine*, vol. 22, no. 4, pp. 70–84, Jul. 2005.

[10] J. Fernández-Madrigal, E. Cruz, J. González, C. Galindo, and J. Blanco, "Application of UWB and GPS Technologies for Vehicle Localization in Combined Indoor-Outdoor Environments," in *Proceedings of the International Symposium on Signal Processing and its Applications*, Sharja, United Arab Emirates, Feb. 2007.

[11] "Real Time Location Systems (RTLS)," Nanotron Technologies GmbH, Berlin, Germany, White paper NA-06-0248-0391-1.02, Apr. 2007.

[12] J. Park and H. Song, "Multilevel Localization for Mobile Sensor Network Platforms," in *Proceedings of the International Multiconference on Computer Science and Information Technology*, vol. 3, Wisla, Poland, Oct. 2008, pp. 711–718.

[13] C. Lam, W. Kuo, C. Liao, Y. Jong, L. Fu, and J. Feng, "An Efficient Hierarchical Localization for Indoor Mobile Robot with Wireless Sensor and Pre-Constructed Map," in *Proceedings of the 5th International Conference on Ubiquitous Robots and Ambient Intelligence (URAI 2008)*, Seoul, South Korea, Nov. 2008.

[14] D. Fox, J. Hightower, and L. Liao, "Bayesian filtering for location estimation," *IEEE Pervasive Computing*, vol. 2, no. 3, pp. 24–33, 2003.

[15] F. Dellaert, D. Fox, W. Burgard, and S. Thrun, "Monte Carlo Localization for Mobile Robots," in *Proceedings of the IEEE International Conference on Robotics and Automation (ICRA99)*, May 1999.

[16] D. Fox, W. Burgard, F. Dellaert, and S. Thrun, "Monte Carlo Localization: Efficient Position Estimation for Mobile Robots," in *Proceedings of the National Conference on Artificial Intelligence (AAAI*, 1999, pp. 343–349.

[17] S. Thrun, W. Burgard, and D. Fox, *Probabilistic Robotics*. Massachusetts USA: The MIT Press, 2006.

[18] P. F. Muir, "Modeling and Control of Wheeled Mobile Robots," Ph.D. dissertation, Carnegie Mellon University, 1988.